

## Codoped ZnO films by a co-spray deposition technique for photovoltaic applications

Bin Zhou, Xiaofei Han and Meng Tao\*

School of Electrical, Computer and Energy Engineering, Arizona State University, Tempe, AZ 85287, USA

(Received November 6, 2014, Revised December 28, 2014, Accepted December 30, 2014)

**Abstract.** A co-spray deposition technique has been developed to bypass a fundamental limitation in the conventional spray deposition technique, i.e., the deposition of metal oxides from incompatible precursors in the starting solution. With this technique, ZnO films codoped with F and Al have been successfully synthesized, in which F is incompatible with Al. Two starting solutions were prepared and co-sprayed through two separate spray heads. One solution contained only the F precursor,  $\text{NH}_4\text{F}$ . The second solution contained the Zn and Al precursors,  $\text{Zn}(\text{O}_2\text{CCH}_3)_2$  and  $\text{AlCl}_3$ . The deposition was carried out at  $500^\circ\text{C}$  on soda-lime glass in air. A minimum sheet resistance,  $55.4 \Omega/\square$ , was obtained for Al and F codoped ZnO films after vacuum annealing at  $400^\circ\text{C}$ , which was lower than singly-doped ZnO with either Al or F. The transmittance for the codoped ZnO samples was above 90% in the visible range. This co-spray deposition technique provides a simple and cost-effective way to synthesize metal oxides from incompatible precursors with improved properties for photovoltaic applications.

**Keywords:** spray deposition; ZnO; doping; transparent conducting oxide

---

### 1. Introduction

Indium tin oxide (ITO) is arguably the best performance transparent conducting oxide (TCO) to date. Some of the problems for ITO include the scarcity of In, which prevents its applications in terawatt solar photovoltaics (Tao *et al.* 2011), and the vacuum deposition processes for ITO such as magnetron sputtering, which are costly (Jarzebski 1982). These problems necessitate a solution-prepared earth-abundant substitute for ITO in solar photovoltaics. ZnO, a naturally n-type semiconductor, has been identified as a promising candidate to replace ITO in solar photovoltaics, due to its advantages of low cost, abundant raw materials, wide bandgap (3.37 eV), and suitable refractive index (2.0 at 600 nm). Undoped ZnO has a resistivity too high for photovoltaic applications and doping is required to reduce its resistivity. N-type doping in ZnO is realized by introducing either a cationic dopant from group IIIA (Al, In, or Ga) into the Zn site or an anionic dopant from group VIIA (mainly F) into the O site. Different deposition processes have been demonstrated for the synthesis of undoped and singly-doped ZnO films such as sputtering (Jeong *et al.* 2003), CVD (Barnes *et al.* 2005), sol-gel (Li *et al.* 2004), electrodeposition (Zhou *et al.* 2012), ionic layer deposition (Lee *et al.* 2013) and spray deposition (Paraguay *et al.* 2000).

---

\*Corresponding author, Professor, E-mail: [meng.tao@asu.edu](mailto:meng.tao@asu.edu)

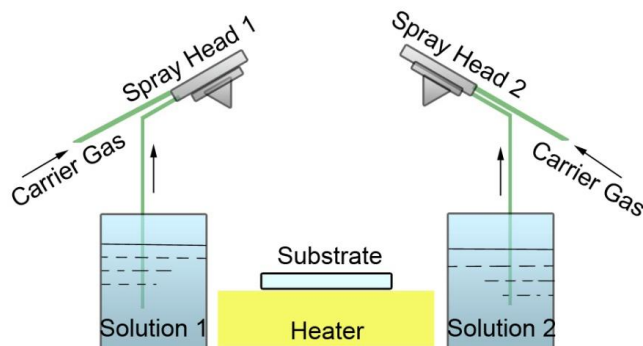


Fig. 1 Schematic of the home-built co-spray deposition setup. There are two containers for two solutions, co-sprayed through two spray heads

Codoping, i.e., simultaneous introduction of two dopants is a possible way to further reduce the resistivity of ZnO due to double doping. This is particularly true when a cationic dopant and an anionic dopant are simultaneously introduced, as they go into different sublattices in ZnO. ZnO films codoped with Mg and Ga, Sn and F, and Al and F have been reported using sputtering (Houng and Chen 2012), CVD (Shin *et al.* 2011), and sol-gel processes (Pan *et al.* 2013). Although spray deposition is a convenient and low-cost process for large-area ZnO films, there have been few reports on codoped ZnO by spray deposition, especially for codoping with a cation and an anion (Snega *et al.* 2013). This may lie with the fundamental limitation in solution-based spray deposition - all the precursors for spray deposition have to be compatible in the same solution and do not react or precipitate in the solution. Taking Al and F codoped ZnO as an example.  $\text{Al}^{3+}$  ions react with  $\text{F}^-$  ions in the same solution resulting in precipitation of insoluble  $\text{AlF}_3$ . This prevents spray deposition of Al and F codoped ZnO.

In this paper we report a new co-spray deposition technique for the synthesis of metal oxides from incompatible precursors. The technique bypasses the problem by preparing two starting solutions and co-spraying them through two spray heads. ZnO films codoped with Al and F, Cr and F, and Fe and F have been successfully demonstrated. Structural, morphological, electrical, and optical properties of codoped ZnO films by spray deposition have been investigated. To the best of our knowledge, no report has appeared in the literature on codoping ZnO in spray deposition with Al and F, Cr and F, or Fe and F. The only report on codoping ZnO in spray deposition involves Mg and F (Snega *et al.* 2013), but the paper did not address the issue of chemical compatibility.

## 2. Experimental

The schematic of the home-built co-spray deposition setup is shown in Fig. 1. It involves two containers for two solutions, with separate liquid feeding and carrier gas lines for two spray heads. The spray heads were model STA-6N-0.5 from Fuso Seiki Co., Ltd. The heater for the substrate in the setup is a hotplate capable of  $540^\circ\text{C}$ , but a different heater more suitable for industrial-scale synthesis of ZnO films can be employed.

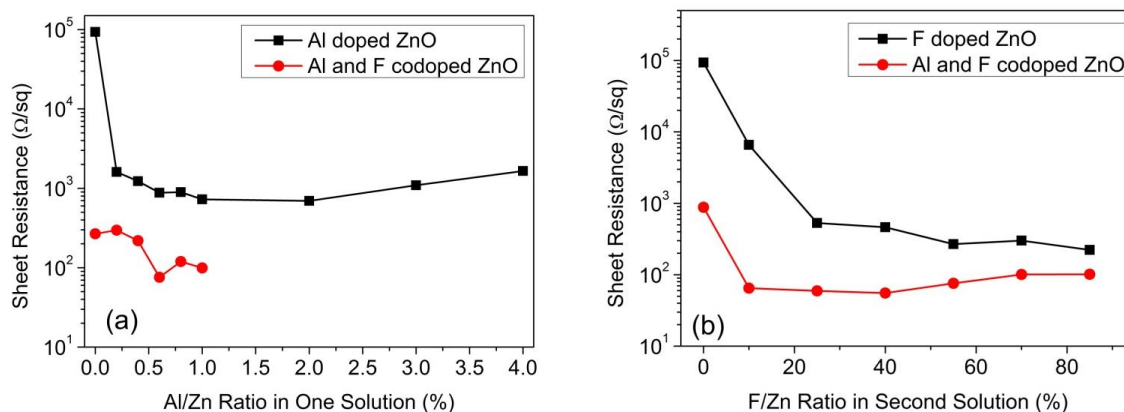


Fig. 2 Sheet resistance of singly-doped and codoped ZnO films as a function of (a) Al/Zn ratio in one solution with a fixed F/Zn ratio of 55% in second solution and (b) F/Zn ratio in second solution with a fixed Al/Zn ratio of 0.6% in first solution

Three pairs of dopants, Al and F, Cr and F, and Fe and F, were selected for codoping in ZnO. Of the two starting solutions, one contained the Zn precursor,  $\text{Zn}(\text{O}_2\text{CCH}_3)_2$ , and the cationic dopant precursor,  $\text{AlCl}_3$ ,  $\text{CrCl}_3$ , or  $\text{FeCl}_3$ . The precursors were dissolved into a mixture of deionized water and ethanol in a volume ratio of 3:2. A few drops of acetic acid were added to prevent precipitation in the solution. In the second solution, the F precursor,  $\text{NH}_4\text{F}$ , was dissolved into a mixture of deionized water and ethanol in the same ratio. The concentration of  $\text{Zn}(\text{O}_2\text{CCH}_3)_2$  was fixed at 0.4 M in one solution. In this paper, the cationic dopant concentration ( $\text{AlCl}_3$ ,  $\text{CrCl}_3$ , or  $\text{FeCl}_3$ ) in one solution and the  $\text{NH}_4\text{F}$  concentration in the other solution are expressed in cation/Zn and F/Zn ratios.

The two solutions were co-sprayed onto a preheated soda-lime glass substrate maintained at 500°C in air. Before deposition, the substrate was ultrasonically cleaned in deionized water, acetone, and deionized water sequentially. The deposition time was 2 min, and the film thickness of Al and F, Cr and F, and Fe and F codoped ZnO films by profilometry was ~0.8 μm, ~0.5 μm, and ~0.6 μm, respectively. The thickness variation of ZnO films with the same dopants was small. Compressed air was used as the carrier gas and the atomization pressure was 30 psi. Post-deposition annealing was performed in a tube furnace at 400°C under 10<sup>-3</sup> torr for 1 h for all the samples.

Optical properties of the samples were characterized using a JASCO V-670 UV/vis spectrophotometer with an integrating sphere. Electrical properties were measured with a Jandel RM3000 four-point probe. Structural properties were investigated with a Panalytical X'Pert Pro X-ray diffractometer (XRD) using the Cu Kα line. Film morphologies were examined with a Hitachi S-4700 field emission scanning electron microscope (SEM). Film thickness was determined using a Bruker Dektak XT surface profilometer.

### 3. Results and discussion

Fig. 2 shows the sheet resistance of Al and F codoped ZnO films as a function of doping

concentrations in the starting solutions. For comparison, the sheet resistance of singly-doped ZnO films, with either Al or F, is also plotted as a function of doping concentration in the solution. Fig. 2(a) shows the effect of Al concentration on sheet resistance, where the F/Zn ratio in the solution is fixed at 55% for codoped samples. For Al singly-doped samples, the sheet resistance decreases with increasing Al/Zn ratio up to 2% and then increases slightly with Al/Zn ratio. This can be explained by substitution of more Al atoms into the Zn site, resulting in more free electrons in the lattice. Without doping, the sheet resistance is on the order of  $10^5 \Omega/\square$ . With Al doping, it drops to  $\sim 10^3 \Omega/\square$ . For Al and F codoped samples, the sheet resistance is on average  $\sim 10$  times lower than Al singly-doped samples into the  $10^2 \Omega/\square$  range. Between 0 – 1% Al/Zn ratio, the sheet resistance of codoped samples decreases first and then increases slightly. The minimum sheet resistance is  $75.8 \Omega/\square$  at 0.6% Al/Zn ratio.

The significant reduction in sheet resistance by codoping is attributed to double doping. The amount of Al which can be incorporated substitutionally into the Zn sublattice is thermodynamically limited by the solid solubility of Al in ZnO. Excess Al likely forms a second phase in ZnO,  $\text{Al}_2\text{O}_3$ , which is an insulator and increases the resistivity of the matrix ZnO. Introducing substitutional F into the O sublattice bypasses the solid solubility of Al and adds more electron donors to the lattice. This double-doping effect by a cation and an anion is unlikely to be matched by two cationic dopants or two anionic dopants. For Al singly-doped samples, the minimum sheet resistance appears at 2% Al/Zn ratio, while for codoped samples, the minimum sheet resistance is at 0.6% Al/Zn ratio. It is suggested that the presence of F in the lattice likely reduces the thermodynamic solubility limit for Al in ZnO.

Fig. 2(b) shows the effect of F concentration on sheet resistance, where the Al/Zn ratio is fixed at 0.6% in one solution for codoped samples. Codoping reduces the sheet resistance of ZnO by a factor of  $\sim 10$  on average. A minimum sheet resistance of  $55.4 \Omega/\square$  is obtained for Al and F codoped samples at Al/Zn ratio of 0.6% and F/Zn ratio of 40% in the starting solutions. For codoped samples, the sheet resistance initially decreases with increasing F/Zn ratio between 0 – 40%. Beyond 40% F/Zn ratio, the sheet resistance increases with F/Zn ratio. The initial reduction of sheet resistance is due to the substitution of O atoms by F atoms leading to a higher free electron concentration. Beyond a certain point, excess F might go into interstitial sites or segregate to grain boundaries, resulting in a high density of defects (Sanchez-Juarez *et al.* 1998), which increases the sheet resistance by carrier scattering.

The selection of Cr and Fe for codoping ZnO with F is because they are earth-abundant and their multiple valences include 3+. Fig. 3 shows the sheet resistance of ZnO films, codoped with Cr and F and with Fe and F, as a function of doping concentrations in the starting solutions. In contrast to Al and F codoped ZnO, Cr doping increases the sheet resistance of Cr and F codoped samples at all Cr concentrations examined, as shown in Fig. 3(a). Obviously, Cr does not act as an electron donor in ZnO, as corroborated by Maldonado *et al.* (2000). As XRD in Fig. 4(c) reveals no new phase other than ZnO, it is suggested that the valence of Cr in the Zn site is  $\text{Cr}^{2+}$  rather than  $\text{Cr}^{3+}$  which does not donate electrons.

Fig. 3(a) also shows the effect of Fe/Zn ratio on sheet resistance of Fe and F codoped ZnO. The sheet resistance initially decreases with increasing Fe/Zn ratio and then increases with further increase in Fe/Zn ratio. The lowest sheet resistance,  $196 \Omega/\square$ , is obtained at Fe/Zn ratio of 0.4% and F/Zn ratio of 55% in the solutions. XRD in Fig. 4(d) detects no other phase other than ZnO in the Fe and F codoped ZnO sample, so the initial decrease in sheet resistance can be attributed to substitution of  $\text{Fe}^{3+}$  into the Zn site. The existence of  $\text{Fe}^{3+}$  in ZnO has been confirmed by Rambu *et al.* (2013). With further increase in Fe/Zn ratio, excess Fe may go into interstitial sites resulting in

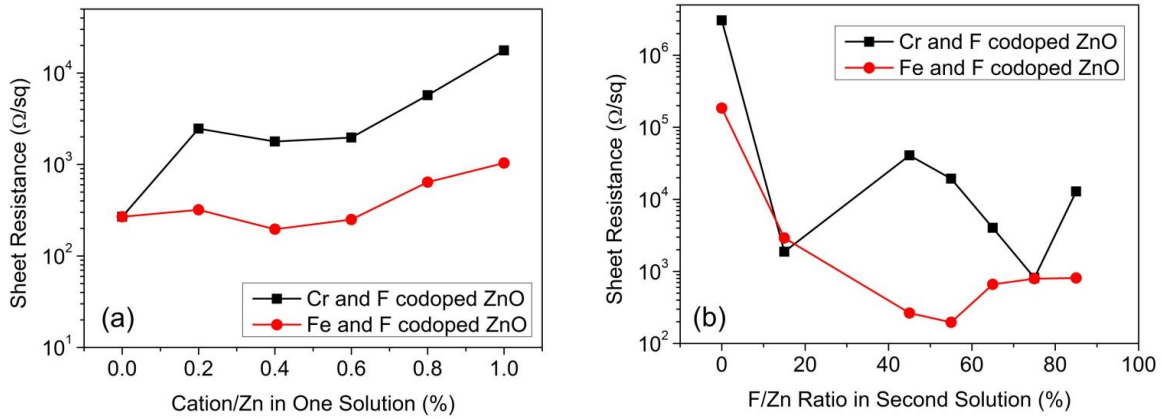


Fig. 3 Sheet resistance of singly-doped and codoped ZnO films as a function of (a) cation/Zn ratio in one solution with a fixed F/Zn ratio of 55 % in second solution and (b) F/Zn ratio in second solution with a fixed cation/Zn ratio of 0.4 % in first solution

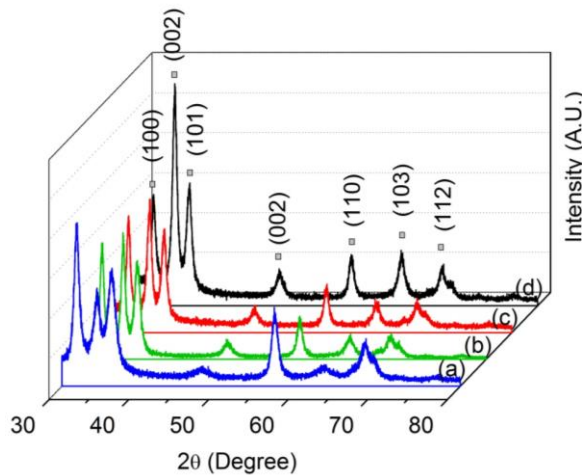


Fig. 4 XRD patterns of (a) undoped ZnO; (b) Al and F codoped ZnO with Al/Zn ratio of 0.6% and F/Zn ratio of 55%; (c) Cr and F codoped ZnO with Cr/Zn ratio of 0.4% and F/Zn ratio 55%; (d) Fe and F codoped ZnO with Fe/Zn ratio 0.4% and F/Zn ratio 55% in the solutions

neutral defects, which increases the sheet resistance by defect scattering. Although not shown in Fig. 3(a), the sheet resistance of Fe singly-doped ZnO film is  $185 \text{ k}\Omega/\square$  at F/Zn ratio of 0.4% and that of F singly-doped ZnO is  $322 \Omega/\square$  at F/Zn ratio of 55%. Fe and F codoped ZnO possesses a much lower sheet resistance at Fe/Zn ratio of 0.4% and F/Zn ratio of 55%, clearly demonstrating the double-doping effect.

Fig. 3(b) shows the effect of F/Zn ratio on sheet resistance of ZnO films codoped with Cr and F and with Fe and F, with Cr/Zn and Fe/Zn ratios fixed at 0.4%. While the Cr and F codoped samples behave irrationally, Fe and F codoped samples have a minimum sheet resistance between 0 – 85% F/Zn ratio.

XRD patterns of undoped, Al and F codoped, Cr and F codoped, and Fe and F codoped ZnO

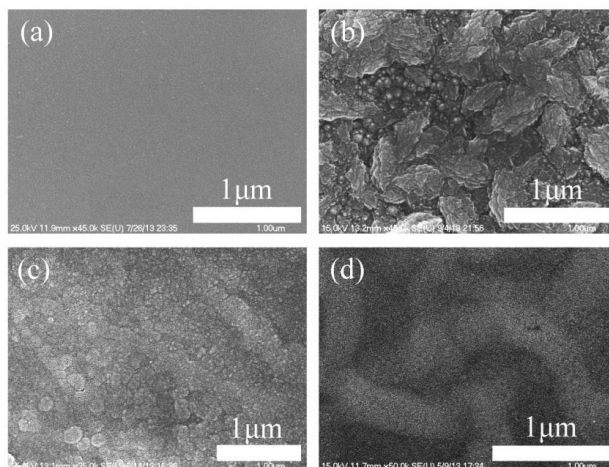


Fig. 5 SEM images of (a) undoped ZnO; (b) Al and F codoped ZnO with Al/Zn ratio of 0.6% and F/Zn ratio 55%; (c) Cr and F codoped ZnO with Cr/Zn ratio 0.4% and F/Zn ratio 55%; (d) Fe and F codoped ZnO with Fe/Zn ratio 0.4% and F/Zn ratio 55% in the solutions

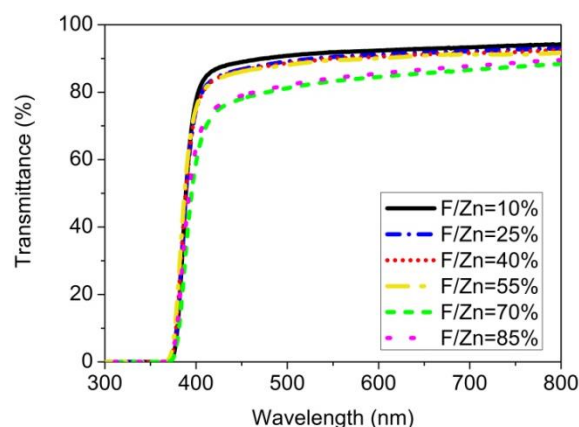


Fig. 6 Total transmittance spectra of Al and F codoped ZnO films as a function of F/Zn ratio in second solution with a fixed Al/Zn ratio of 0.6 % in first solution. The F/Zn ratio varies from 10% to 85%

samples are shown in Fig. 4. The F/Zn ratio for all the codoped samples is 55%. The Al/Zn ratio is 0.6%, while the Cr/Zn and Fe/Zn ratios are 0.4%. All the samples were deposited at 500°C and then annealed in vacuum. All the samples show the same diffraction peaks, although the intensities of the peaks vary. Diffraction peaks at 31.7°, 34.3°, 36.2°, 47.6°, 56.5°, 62.9°, and 67.8° correspond to wurtzite ZnO(100), (002), (101), (102), (110), (103), and (112), respectively. Only ZnO is detected for all the samples, and all the samples are polycrystalline films. It is noted that undoped ZnO (Fig. 4 (a)) has a preferential (100) orientation and Fe and F codoped ZnO (Fig. 4 (d)) has a preferential (002) orientation. Al and F codoped ZnO (Fig. 4(b)) and Cr and F codoped ZnO (Fig. 4(c)) show no preferential orientation. Introduction of two dopants may change the surface energy of ZnO leading to different orientations (Morinaga *et al.* 1997).

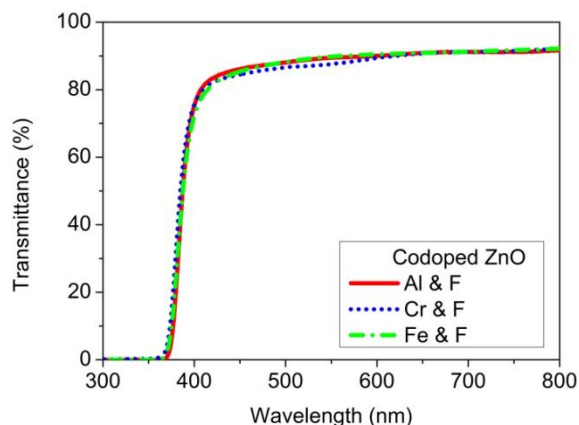


Fig. 7 Total transmittance spectra of (a) Al and F codoped ZnO with Al/Zn ratio of 0.6% and F/Zn ratio 55%; (b) Cr and F codoped ZnO with Cr/Zn ratio 0.4% and F/Zn ratio 55%; (c) Fe and F codoped ZnO with Fe/Zn ratio 0.4% and F/Zn ratio 55% in the solutions

Surface morphology of the samples in Fig. 4 is presented in Fig. 5. All the samples show continuous films with granular structures. Undoped ZnO has the smallest grain size, while Al and F codoped ZnO has the largest grain size. Fig. 6 is the total transmittance spectra, measured with an integrating sphere, of Al and F codoped ZnO samples with a fixed Al/Zn ratio of 0.6% in one solution and varying F/Zn ratio in second solution. The transmittance of Al and F codoped samples decreases with increasing F/Zn ratio. When the F/Zn ratio increases from 55% to 70%, the transmittance in the visible range decreases sharply from ~90% to ~80%. This limits the F concentration in ZnO. Fig. 7 is the total transmittance spectra of the Al and F, Cr and F, and Fe and F codoped samples in Fig. 4. All the samples show similar transmittance, as they are prepared with the same F/Zn ratio, 55%, and a low cationic concentration. The transmittance is above 90% in the visible range for all the samples.

#### 4. Conclusions

A co-spray deposition technique is demonstrated, which is particularly suitable for depositing metal oxides from incompatible precursors. ZnO films codoped with Al and F, Cr and F, or Fe and F are reported, where the F precursor is in a separate solution from the Zn and cationic dopant precursors. The two solutions are co-sprayed through two spray heads. In Cr and F codoped ZnO, Cr does not act as an electron donor. Al and F codoped ZnO and Fe and F codoped ZnO both show double-doping effects which result in significantly lower sheet resistance than singly-doped ZnO with either Al, Fe, or F. Al and F codoped ZnO films possess the lowest sheet resistance of all the samples, which is  $55.4 \Omega/\square$ , deposited from solutions with Al/Zn ratio of 0.6% and F/Zn ratio of 40%. The total transmittance for all the codoped ZnO samples is above 90% in the visible range. This co-spray deposition technique provides a simple and cost-effective way to synthesize metal oxides from incompatible precursors with improved properties for photovoltaic applications.

## References

- Barnes, T.M., Leaf, J., Fry, C. and Wolden, C.A. (2005), "Room temperature chemical vapor deposition of c-axis ZnO", *J. Cryst. Growth*, **274**(3-4), 412-417.
- Houng, B. and Chen, H.B. (2012), "Investigation of AlF<sub>3</sub> doped ZnO thin films prepared by RF magnetron sputtering", *Ceram. Int.*, **38**(1), 801-809.
- Jarzebski, Z.M. (1982), "Preparation and physical properties of transparent conducting oxide films", *Phys. Stat. Sol. A*, **71**(1), 13-41.
- Jeong, S.H., Lee, J.W., Lee, S.B. and Boo, J.H. (2003), "Deposition of aluminum-doped zinc oxide films by RF magnetron sputtering and study of their structural, electrical and optical properties", *Thin Solid Film.*, **435**(1-2), 78-82.
- Lee, P.Y., Chang, S.P. and Chang, S.J. (2013), "Synthesis and optical properties of ZnO thin films prepared by SILAR method with ethylene glycol", *Adv. Nano Res.*, **1**(2), 93-103.
- Li, H., Wang, J., Liu, H., Yang, C., Xu, H., Li, X. and Cui, H. (2004), "Sol-gel preparation of transparent zinc oxide films with highly preferential crystal orientation", *Vacuum*, **77**(1), 57-62.
- Maldonado, A., de la Olvera, M., Asomoza, R. and Tirado-Guerra, S. (2000), "Characteristics of ZnO:Cr thin films deposited by spray pyrolysis", *J. Vac. Sci. Technol. A*, **18**(5), 2098-2101.
- Morinaga, Y., Sakuragi, K., Fujinura, N. and Ito, T. (1997), "Effect of Ce doping on the growth of ZnO thin films", *J. Cryst. Growth*, **174**(1-4), 691-695.
- Pan, Z., Zhang, P., Tian, X., Cheng, G., Xie, Y., Zhang, H., Zeng, X., Xiao, C., Xiao, C., Hu, G. and Wei, Z. (2013), "Properties of fluorine and tin co-doped ZnO thin films deposited by sol-gel method", *J. Alloy. Compd.*, **576**(5), 31-37.
- Paraguay, F., Morales, J., Estrada, W., Andrade, E. and Miki-Yoshida, M. (2000), "Influence of Al, In, Cu, Fe and Sn dopants in the microstructure of zinc oxide thin films obtained by spray pyrolysis," *Thin Solid Film.*, **366**(1-2), 16-27.
- Rambu, A.P., Nica, V. and Dobromir, M. (2013), "Influence of Fe-doping on the optical and electrical properties of ZnO films", *Superlattice Microst.*, **59**, 87-96.
- Sanchez-Juarez, A., Tiburcio-Silver, A., Ortiz, A., Zironi, E. P. and Rickards, J. (1998), "Electrical and optical properties of fluorine-doped ZnO thin films prepared by spray pyrolysis", *Thin Solid Film.*, **333**(1-2), 196-202.
- Shin, S.W., Kim, I.Y., Lee, G.H., Agawane, G.L., Mohokar, A.V., Heo, G., Kim, J.H. and Lee, J.Y. (2011), "Design and growth of quaternary Mg and Ga codoped ZnO thin films with transparent conductive characteristics", *Cryst. Growth Des.*, **11**(11), 4819-4824.
- Snega, S., Ravichandran, K. and Begum, N.J. (2013), "Enhancement in the electrical and antibacterial properties of sprayed ZnO films by simultaneous doping of Mg and F", *J. Mater. Sci.: Mater. Electron.*, **24**(1), 135-141.
- Tao, C.S., Jiang, J. and Tao, M. (2011), "Natural resource limitations to terawatt-scale photovoltaic solar cells", *Solar Energy Mater. Solar Cell.*, **95**(12), 3176-3180.
- Zhou, B., Han, X., Feng, Q. and Tao, M. (2012), "A greener electrodeposition recipe for ZnO films in terawatt photovoltaics", *Thin Solid Film.*, **520**(22), 6730-6733.